Available online at www.sciencedirect.com
ScienceDirect
Computational Materials Science 42 (2008) 659–663
COMPUTATIONAL MATERIALS SCIENCE
www.elsevier.com/locate/commatsci

Analytical algorithm for Equivalent Crystal Theory

Fredy R. Zypman [a,*], John Ferrante [b]

[a] Yeshiva University, Department of Physics, New York, NY 10033, United States
[b] NASA-Glenn, Stop 23-2, 21000 Brookpark Road, Cleveland, OH 44135, United States

Received 3 August 2007; received in revised form 25 September 2007; accepted 30 September 2007
Available online 19 November 2007

Abstract

Equivalent crystal theory (ECT) is a semi-empirical technique used for the calculation of defect energetics in metals and semiconductors. The implementation of the method involves the solution of transcendental equations. Although this is not a problem for simple defects, for complex defects, Monte Carlo and molecular dynamics calculations in large systems, it could be the speed-determining limitation in a calculation. In this paper we propose a procedure for bypassing this step and obtaining the desired result directly. The form of the particular transcendental equations suggest a different approach, namely, the equation can be cast in the form of the Lambert function that can be readily evaluated from standard routines. We test this scheme by evaluating the surface energies for a variety of metallic elements and by standard numerical approaches, and demonstrate that they agree to within a few ppm.

PACS: 61.66.Bi; 61.72.Bb; 61.82.Bg

Keywords: Equivalent crystal theory; Lambert function; Computational speed optimization; Semi-empirical methods

1. Introduction

Equivalent crystal theory (ECT) [1] belongs to the class of semi-empirical quantum algorithms used to evaluate the energies of metallic and semiconductor atomic aggregates. It has been applied to determining the energies of crystal defects [2], the energetics of alloys using the Bozzolo–Ferrante–Smith (BFS)–ECT method [3,4] and more recently to study charge transfer in metal nano-clusters [5]. Of particular interest is the calculation of surface energies. In ECT like in other semi-empirical methods, surface energies typically agree with ab initio values within 20% – see for example Skriver et al. [6] for ab initio results, Daw for embedded atom method [7], and Mehl and Papaconstantopoulos for tight binding [8]. By allowing for charge transfer, the agreement can be improved to below 20% as shown in Ref. [5]. In the present paper, our objective is to improve the computational speed of the ECT algorithm. ECT as originally formulated, although giving outstanding agreement for the high-density planes [9], tends to overestimate the anisotropy ratio for higher index planes. A complete discussion of this issue is presented in Ref. [9].

In ECT the total energy of a collection of atoms in a defect is the sum of individual energy contributions $U(a_{eq})$, where a_{eq} is called equivalent lattice parameter and $U(a_{eq})$ is explicitly given by the Universal Binding Energy Relation (UBER) [10] which is simply parameterized in terms of physically known constants in the Rydberg function. In ECT an atom near a defect is viewed as sensing a reduced or increased electron density. This condition is then interpreted as a point on the UBER in terms of an expanded or contracted perfect crystal. Perturbation theory is used to obtain the equivalent lattice parameter of the expanded or contracted crystal, a_{eq}, in terms of a_0, the lattice parameter corresponding to the perfect crystal. Once a_{eq} is known, the energy the atom near the defect is obtained from that point on the UBER. The value of a_{eq} is obtained in terms of a_0 from the inversion of the basic

* Corresponding author.
E-mail address: zypman@yu.edu (F.R. Zypman).

0927-0256/$ - see front matter © 2007 Elsevier B.V. All rights reserved.
doi:10.1016/j.commatsci.2007.09.017

ECT transcendental equation that is given in Section 2. Although conceptually simple, the inversion process represents the computational time limiting step in the implementation of the algorithm. In this paper we present an analytical expression to invert this equation that reduces the computation speed. In Section 2 we state the problem. In Section 3, we present the exact solution to the approximate problem when the atomic electron density decays fast enough that only first near neighbors play a role in the calculation. In Section 4 we study the location of the maximum of the density curve. This is necessary to understand the region of parameter space in which ECT operates. In Section 5, we present the general solution. In Section 6, we perform a test of the method: we evaluate the surface energy formation for a variety of elements and compare with the standard approach. Finally, Section 7 presents conclusions.

2. The problem

The implementation of ECT involves a perturbation equation that determines the energy of a solid with a defect in terms of a perfect crystal of the same substance expanded or contracted from the equilibrium lattice parameter to a new, "equivalent" lattice parameter. This procedure is equivalent to finding and embedding electron density ρ. A typical atom at a given location is embedded in a density ρ produced by the electronic charge density of the remainder atoms in the system. The, yet unknown, equivalent nearest-neighbor distance, R_{eq}, satisfies

$$N_1 R_{eq}^p e^{-\alpha R_{eq}} + N_2 (cR_{eq})^p e^{-(\alpha+\frac{1}{\gamma})cR_{eq}} = \rho \tag{1}$$

where N_1 is the number of nearest-neighbors in the minimum energy crystal structure corresponding to that atom, N_2 is the number of next-nearest- neighbors, c is the ratio of the next-nearest-neighbor distance to the nearest- neighbor distance, and α and λ are known material-dependent constants. In many applications of ECT to evaluate defect formation energies, ρ, on the right-hand side of (1), is written in a form similar to the left-hand side. For example, the density produced by neighbors on an atom next to a vacancy is $\rho = N_1' R_0^p e^{-\alpha R_0} + N_2' (cR_0)^p e^{-(\alpha+\frac{1}{\lambda})cR_0}$ where $N_1' = N_1 - 1$ and $N_2' = N_2$ because the atom in question loses one next nearest-neighbor (where the vacancy is located) and no second near neighbor. In this example, the lattice is unrelaxed and, consequently R_0 represents the nearest-neighbor distance of the perfect crystal. This shows explicitly that R_{eq} is the unknown in Eq. (1). Once R_{eq} is obtained, ECT uses this value in the UBER function $U(a_{eq})$. The corresponding energy cost is then $U(a_{eq}) - U(a_0)$.

The general problem is to find the function

$$R_{eq} = G(\rho) \tag{2}$$

Eq. (1) can be cast in dimensionless form by defining $y \equiv \alpha R_{eq}$,

Table 1
Smallest values of y and corresponding γ values for various elements

	$y_{minimum}$	γ	$n_{21}c^p e^{-\gamma y}$
Al	3.537	1.126	0.037
Cu	5.282	1.044	0.016
Ag	6.960	0.975	0.009
Au	8.579	0.906	0.007
Ni	5.282	1.032	0.017
Pd	6.960	1.002	0.007
Pt	8.579	0.882	0.008

Table 2
ECT equivalent lattice parameter, and relative difference between Lambert evaluation and Newton–Raphson method

	a_{eq} (Å)	$\frac{a_{Lambert}-a_{numerical}}{a_{numerical}}$
Al	4.74	4×10^{-7}
Cu	4.33	9×10^{-8}
Ag	4.81	2×10^{-8}
Au	4.60	1×10^{-9}
Ni	4.21	2×10^{-7}
Pd	4.52	4×10^{-9}
Pt	4.42	2×10^{-9}

$$y^p e^{-y} + \frac{N_2}{N_1} c^p y^p e^{-(1+\frac{1}{\alpha\lambda})cy} = \frac{\rho\alpha^p}{N_1} \tag{3}$$

Finally, introducing $\left(1+\frac{1}{\alpha\lambda}\right)c - 1 \equiv \gamma$, $\frac{N_2}{N_1} \equiv n_{21}$, $\frac{\rho\alpha^p}{N_1} \equiv x$,

$$y^p e^{-y}(1 + n_{21} c^p e^{-\gamma y}) = x \tag{4}$$

The constant $\alpha\lambda$ is about unity or larger, and $c > 1$, thus $\gamma > 0$. This is a conservative lower bound for γ. By using appropriate values from Tables 1 and Table 2 in reference [1], one finds the physical constraint $n_{21}c^p e^{\gamma y} < 0.04$. This will be proved at the end of Section 4, in Table 1.

Thus, in Eq. (4), the second term inside the parenthesis is much smaller than unity, a fact that will be used later. The rest of the paper is devoted to build the inverse function $y = G(x)$.

3. Solution for large γ

Inside the parenthesis in Eq. (4), as mentioned at the end of last section, the first term dominates. In fact, in many real applications the second term is dropped [11] and the problem reduces to finding the roots of

$$y^p e^{-y} = x \tag{5}$$

Besides, understanding the solution to (5) will help afterward in obtaining a solution for finite γ.

Fig. 1 shows Eq. (5) graphically, and illustrate the appearance of two roots: one to the left of the maximum that corresponds to a lattice parameter smaller than a_0, and one to the right with lattice parameter larger than a_0. For intrinsic crystal defects (vacancies, divacancies, dislocations, surfaces, steps) the real local density never increases as compared with the perfect crystal and thus, the physically acceptable root is the second one (y_2 in the

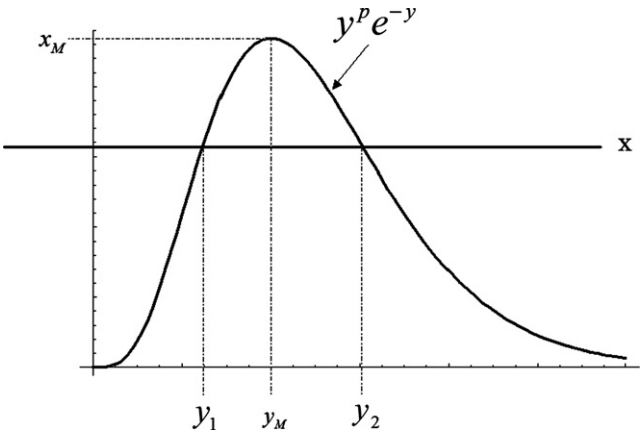

Fig. 1. Intersection of the real reduced density x, and the equivalent density for $\gamma \to \infty$.

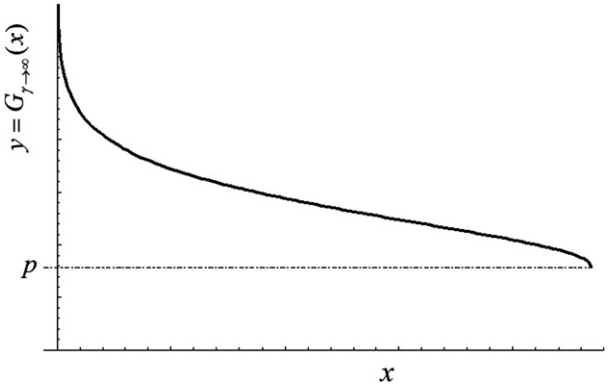

Fig. 2. Equivalent reduced lattice parameter y as a function of the reduced local density x.

figure). If we were treating interstitial defects, then the solution would be the smaller root and, in what follows we would use the other branch of Lambert's function.

Eq. (5) is equivalent to

$$\left(-\frac{y}{p}\right)e^{\left(-\frac{y}{p}\right)} = -\frac{x^{\frac{1}{p}}}{p} \tag{6}$$

and has the solution

$$y = -pW_{-1}\left(-\frac{x^{\frac{1}{p}}}{p}\right) \tag{7}$$

where W_{-1} is the Lambert function [12,13]. This solution is plotted in Fig. 2. The sub index "−1" labels the branch: the Lambert function has an infinite number of complex branches, with only two purely real, the branches known as "0" and "−1". The branch "0" gives the root y_1 in Fig. 1, corresponding to increase in density due for example to an interstitial.

4. Location of the maximum of the density curve

Call (y_M, x_M) the point corresponding to the maximum attainable density (Fig. 1). We will show that $y_M \approx p$ and moreover, we will find y_M (and the corresponding x_M from Eq. (4)).

The location y_M is found by setting $\left[\frac{dx}{dy}\right]_{y=y_M}$ to zero from Eq. (4) thus,

$$p - y_M + n_{21}c^p e^{-\gamma y_M}[p - (1+\gamma)y_M] = 0 \tag{8}$$

This provides an implicit function y_M of γ. Let us write the solution to (8) as

$$y_M = \Omega(\gamma) \tag{9}$$

We will derive some properties of $\Omega(\gamma)$ from Eq. (8). First, if $\gamma = 0$ then $y_M = p$. Taylor-expansion of (8) to first order in γ and $(y_M - p)$ provides

$$\Omega(\gamma) \approx p - \frac{n_{21}c^p}{1 + n_{21}c^p}p\gamma \quad \text{for } \gamma \approx 0 \tag{10a}$$

Second, also from Eq. (8), when $\gamma \to +\infty$, $y_M \to p^-$. In that limit, the term in Eq. (8) containing the exponential is small and can be treated perturbatively leading to

$$\Omega(\gamma) \approx p - n_{21}c^p e^{-\gamma p}p\gamma \quad \text{for } \gamma \to +\infty \tag{10b}$$

A sketch of $\Omega(\gamma)$ is shown in Fig. 3. That particular graph is for FCC Ni or Cu, but the most important features are general, namely: that Eq. (10) is satisfied; that there is a single minimum; that $\frac{d\Omega}{d\gamma}$ remains small for all values of γ.

Next, we obtain γ_m and y_{Mm} as defined in Fig. 3. Eq. (8) cannot be solved analytically for y_M, but it can be solved for γ,

$$\gamma \equiv \Omega^{-1}(y_m) = \frac{1}{y_M}\left[p - y_M - W_0\left(-\frac{(p-y_M)e^{p-y_M}}{n_{21}c^p}\right)\right] \tag{11}$$

The point y_{Mm}, can now be found from (11),

$$\frac{1}{\left(\frac{d\Omega^{-1}(y_M)}{dy_M}\right)_{y_M = y_{Mm}}} = 0 \tag{12}$$

And, explicitly,

$$(p - y_{Mm})y_{Mm}^2\left[1 + W_0\left(\frac{(y_{Mm}-p)e^{p-y_{Mm}}}{n_{21}c^p}\right)\right] = 0 \tag{13}$$

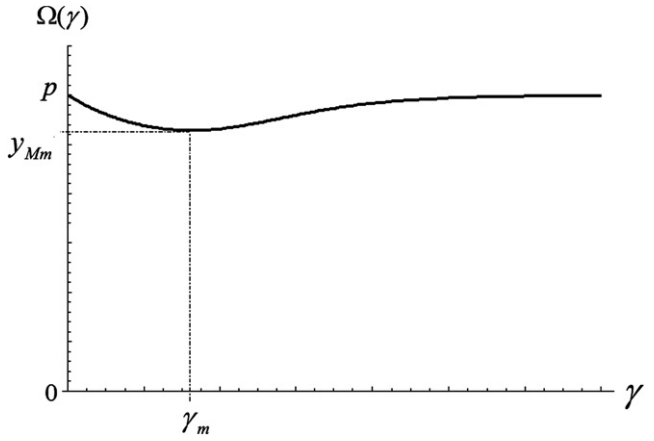

Fig. 3. Location of the maximum $y_M = \Omega(\gamma)$ of the density curve as a function of γ.

Since $y_{Mm} \neq 0$, the only non-trivial solution is for $W_0\,() = -1$. This happens when the argument of the Lambert function is $-1/e$, then,

$$y_{Mm} = p - W_0\left(\frac{n_{21}c^p}{e}\right) \tag{14}$$

This value is the smallest possible y (we called it y_{minimum} in Section 2) and was used to evaluate the entries in Table 1.

5. Solution for finite γ

When $\gamma \to +\infty$ we already obtained,

$$y = -pW_{-1}\left(-\frac{x^{\frac{1}{p}}}{p}\right) \quad \gamma \to +\infty \tag{7}$$

For any γ, Eq. (4) is equivalent to

$$(-y/p)\mathrm{e}^{(-y/p)} = -\frac{1}{p}\left(\frac{x}{1+n_{21}c^p\mathrm{e}^{-\gamma y}}\right)^{1/p} \tag{15}$$

This does not render simply a solution in terms of the Lambert function because y also appears on the right-hand side. However, since $n_{21}c^p\mathrm{e}^{\gamma y} \ll 1$, Eq. (15) can be solved efficiently by recurrence. In the physical cases of interest, $n_{21}c^p\mathrm{e}^{\gamma y} \leqslant 0.04$ and thus a first order solution should suffice. Thus we use (7) on the right-hand side of (15) which can then be readily solved for y

$$y = -pW_{-1}\left[-\frac{1}{p}\left(\frac{x}{1+n_{21}c^p\exp\left(\gamma pW_{-1}\left(-\frac{x^{\frac{1}{p}}}{p}\right)\right)}\right)^{1/p}\right] \tag{16}$$

It is interesting to notice that the limit $\gamma \to 0$ in Eq. (4) can be solved exactly and provides

$$y = -pW_{-1}\left(-\frac{1}{p}\left(\frac{x}{1+n_{21}c^p}\right)^{1/p}\right) \quad \gamma \to 0 \tag{17}$$

This solution is also included in (16) when $\gamma \to 0$.

The two limiting solutions, for large and small γ are shown in Fig. 4. Eq. (16) then serves as an intermediate solution between those two limits.

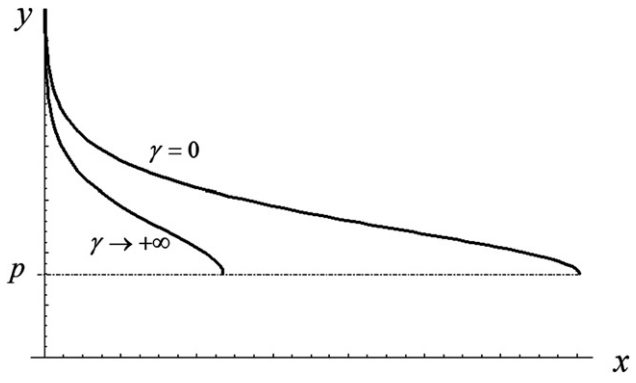

Fig. 4. Solutions $y(x)$ for the two extreme cases, 0 and $+\infty$.

Table 3
Surface energy formation energy, and relative discrepancy between using this algorithm and the standard one

	$E_{\text{effective}}$ (eV/atom)	$\frac{E_{\text{Lambert}}-E_{\text{numerical}}}{E_{\text{numerical}}}$
Al	0.73	3×10^{-6}
Cu	0.98	5×10^{-7}
Ag	0.84	1×10^{-7}
Au	0.89	1×10^{-8}
Ni	1.22	1×10^{-6}
Pd	1.10	3×10^{-8}
Pt	1.31	2×10^{-8}

6. Benchmark: surface energies

We test the scheme developed here to find the surface energy of (100) planes of various elements using Equivalent Crystal Theory. We first solve Eq. (4) both numerically (Newton–Raphson method) and by the evaluation of the Lambert function as explained above. For the real density of the (100) plane, we notice that a typical surface atom loses 4 next near neighbors (out of 12 in bulk) and 1 s near neighbor (out of 6). Then $\rho = 8R_0^p\mathrm{e}^{-\alpha R_0} + 5(cR_0)^p\mathrm{e}^{-(\alpha+\frac{1}{\chi})cR_0}$, with $R_0 = \frac{a_0}{\sqrt{2}}$. The solution to (4) gives y, which in turn gives $R_{\text{eq}} \equiv \frac{a_{\text{eq}}}{\sqrt{2}}$. The equivalent lattice parameter is given in Table 2 with three significant figures, consistent with the original ECT work. The discrepancy between the standard procedure for root finding and the use of the Lambert function as proposed here is given in the same table, as a relative difference. The difference remains well below one part per million.

We use the R_{eq} just described to evaluate the surface energy formation. As described in the original ECT paper, this is done by evaluating the *Universal Binding Energy Relation* in the surface-terminated bulk and in the reference bulk, and then calculating their difference. The results are given in Table 3. All values agree within 3 ppm.

7. Conclusions

We proposed in this paper a new computational algorithm to obtain the equivalent lattice parameter in ECT. The main result is the replacement of the time consuming root-finding section for the direct evaluation of an analytical expression involving the Lambert function. The Lambert function is today easily accessible through standard mathematical packages [14]. We tested our algorithm against the (100) surface energy for a variety of elements. Both, the equivalent lattice parameter, and the surface energy agree with the standard approach to within a few parts per million, well above the discrimination needed in ECT implementations.

Acknowledgment

Work supported by Research Corporation through Grant CC5786.

References

[1] J. Smith, T. Perry, A. Banerjea, J. Ferrante, G. Bozzolo, Phys. Rev. B 44 (1991) 6444.
[2] S.V. Khare, T.L. Einstein, Surf. Sci. 314 (1994) L857–L865.
[3] G. Bozzolo, J. Ferrante, J.R. Smith, Phys. Rev. B 45 (1992) 493–496.
[4] G. Bozzolo, J.E. Garcés, R.D. Noebe, D. Farías, Nanotechnology 14 (2003) 939–945.
[5] A.I. Frenkel, L.D. Menard, P. Northrup, J.A. Rodriguez, F. Zypman, D. Glasner, S.-P. Gao, H. Xu, J.C. Yang, R.G. Nuzzo, in: B. Hedman, P. Pianetta (Eds.), X-ray Absorption Fine Structure—XAFS13, vol. 882, American Institute of Physics, 2007, pp. 749–751.
[6] L. Vitos, A.V. Ruban, H.L. Skriver, J. Kollár, Surf. Sci. 411 (1998) 186–202.
[7] M.S. Daw, Phys. Rev. B 39 (1989) 7441–7452.
[8] M.J. Mehl, D.A. Papaconstantopoulos, Phys. Rev. B 54 (1996) 4519–4530.
[9] A.M. Rodríguez, G. Bozzolo, J. Ferrante, Surf. Sci. 289 (1993) 100–126.
[10] J.H. Rose, J. Ferrante, J.R. Smith, Phys. Rev. Lett. 47 (1981) 675–678.
[11] G. Bozzolo, J. Ferrante, A.M. Rodriguez, J. Comput. Aid. Mater. Des. 1 (1993) 285–304.
[12] F. Chapeau-Blondeau, IEEE Trans. Signal Proc. 50 (2002) 2160–2165.
[13] B. Hayes, American Scientist 93 (2005) 104–108.
[14] S. Wolfram, Mathematica, Addison-Wesley, Redwood City, 1988, In Mathematica, the Lambert function is invoked with Product Log..